Springer

Journal of Mechanical Science and Technology 23 (2009) 739~749

Journal of Mechanical Science and Technology

www.springerlink.com/content/1738-494x
DOI 10.1007/s12206-008-1107-0

A study on the MHD (magnetohydrodynamic) micropump with side-walled electrodes †

Sangsoo Lim and Bumkyoo Choi*

Department of Mechanical Engineering, Sogang University, Seoul, 121-742, Korea

(Manuscript Received June 14, 2007; Revised August 29, 2008; Accepted November 17, 2008)

Abstract

This paper presents the continuous flow MHD(magnetohydrodynamic) micropump with side walled electrodes using Lorentz force, which is perpendicular to both magnetic and electric fields, for the application of microfluidic systems. A theoretically simplified MHD flow model includes the theory of fluid dynamics and electromagnetics and it is based upon the steady state, incompressible and fully developed laminar flow theory. A numerical analysis with the finite difference method is employed for solving the velocity profile of the working fluid across the microchannel under various operation currents and magnetic flux densities. In addition, the commercial CFD code called CFD-ACE has been utilized for simulating the MHD micropump. When the program was run(CFD-ACE), the applied current and magnetic flux density were set to be the variables that affected the performance of the MHD micropump. The MHD micropump was fabricated by using MEMS technology. The performance of the MHD micropump was obtained by measuring the flow rate as the applied DC current was changed from 0 to 1mA at 4900 and 3300 Gauss for the electrodes with the lengths of 5000, 7500 and 10000 ㎛, respectively. The experimental results were compared with the analytical and the numerical results. In addition, with the theoretical analysis and the preliminary experiments, we propose a final model for a simple and new MHD micropump, which could be applicable to microfluidic systems.

Keywords: Micropump; Microfluidic; MHD(magnetohydrodynamic); MEMS; μ-TAS; CFD

1. Introduction

Recently, the research and development of μ-TAS (micro total analysis systems) are being performed worldwide. Especially, in the chemical, medical, and biological fields, μ-TAS, which is being developed to promote development of new material and analysis of various kinds of samples and reagents, is a microscopic device capable of analyzing and processing the substances into micro-scale units simultaneously. It is expected to bring a new revolution in analysis and synthesis fields. It can be possible by the use of microscopic devices, which decreases the consumption of reagents so that it can reduce the costs for the analysis. It also helps with diminishing the discharge of environmentally harmful substances caused from the analysis. At the same time, it facilitates the automation to shorten the analysis time. In such a μ-TAS, all functions necessary to analyze samples and reagents are integrated into a single microfluidic substrate. In the microfluidic system, pumping is required to transport samples and reagents for biological or chemical analysis from one point to another. What makes such a microfluidic system possible may be the fact that micropumps can control the small volume of fluids precisely in microchannels and regulate it effectively. Therefore, micropumps are the most commonly employed components in the microfluidic systems.

Pumps generally fall into two major categories: (1)

† This paper was recommended for publication in revised form by Associate Editor Seungbae Lee
* Corresponding author. Tel.: +82 2 705 8639, Fax.: +82 2 712 0799.
E-mail address: bkchoi@sogang.ac.kr.

displacement pumps, which exert pressure forces on the working fluid through one or more moving boundaries and (2) dynamic pumps, which continuously add energy to the working fluid in a manner that increases either its momentum (as in the case of centrifugal pumps) or its pressure directly (as in the case of electroosmotic and elecrohydrodynamic pumps). Momentum added to the fluid in a displacement pump is subsequently converted into pressure by external fluidic resistance. Many displacement pumps operate in a periodic manner, incorporating some means of rectifying periodic fluid motion to produce net flow. Such periodic displacement pumps can be further broken down into pumps that are based on reciprocating motion, as of a piston or a diaphragm, and pumps that are based on rotary elements such as gears or vanes. The majority of reported micropumps are reciprocating displacement ones in which the moving surface is a diaphragm. These are called membrane pumps or diaphragm pumps. Dynamic pumps include centrifugal pumps, which are typically ineffective at low Reynolds numbers and have only been miniaturized to a limited extent, as well as pumps in which an electromagnetic field interacts directly with the working fluid to produce pressure and flow (electrohydrodynamic pumps, electroosmotic pumps and magnetohydrodynamic pumps) and acoustic-wave micropumps. A common property of these micropumps is the simplicity of the microstructures involved, as no mechanically moving parts are required. The performance is, however, in many cases strongly influenced by a number of fluid properties, which limits a certain principle to a small class of fluids. The EHD principle of fluid transport was proposed first around 1960 and picked up 30 years later by Bart et al.[2] and Richter et al.[3,4] for their electrohydrodynamic micropumps. They used the EHD induction effect, i.e. the generation and movement of induced charges at a fluid-fluid or fluid-solid boundary layer and the EHD injection effect which is based on the electrochemical formation and movement of charged ions. The electrokinetic micropump is the basis of capillary microelectrichromatography which has seen a tremendous progress in science as well as in commercialization during the last several years, mainly pushed by the concept of the lab on a chip. RF and ultrasonic pumping exploit the dragging force of a progressive mechanical wave[5] or the quartz wind of a vertically oscillating surface[6] which are excited at a liquid-solid interface, e.g. the sidewall or the end wall of a microchannel. Centrifugal pumping uses the centrifugal force present in a rotating microchannel system (usually integrated into a disk) to transport fluid from the centre to the perimeter[9].

MHD (Magnetohydrodynamic) pumping, which uses the Lorentz effect, based on the injection of an electric current into two electrodes located at sidewalls facing each other in a microchannel. This charge injection generates a transversal ionic current in the microchannel, which is simultaneously subjected to a magnetic field oriented at an angle of 90° to the current direction and microchannel axis. The Lorentz force acting on the ionic current in the solution will then generate a fluid flow in the microchannel direction. This pumping principle is also bidirectional by nature, as a flow reversal is easily achieved by a reversal of the electric current or the magnetic field vector. Typical MHD micropumps can generate only small values for pump rate and achievable pressure, e.g. 63 $\mu\ell$/min and 1.8 mbar, respectively, for the device described in [7] and do strongly depend on the ionic conductivity of the pumped medium. Electrolytic bubble generation at the injection electrodes can easily occur with DC operation. This problem has been solved with an MHD pump with AC current injection which additionally uses an electromagnet instead of a permanent magnet. By driving both the magnet coil and the current injector from synchronized AC sources, the Lorentz vector and, hence, the direction of fluid flow remains in the same direction. Choosing the operation frequency high enough will prevent the electrolytic formation of gas bubbles. While representing a disturbing effect in MHD pumps, the electrolytic generation of gas bubbles can also be exploited as an excellent and simple actuation principle to realize high precision dosing systems. This concept has found its first applications in drug delivery and is well illustrated in the publication of Böhm[8]. He used a reservoir filled with an electrolyte and two immersed electrodes to generate gas bubbles by current injection. The corresponding volume increase generates a continuous or step-by-step displacement in an adjacent meander, which carries the fluid to be dispensed. By a closed-loop control of the gas generation process this dosing system is able to deliver fluid quantities as small as 100 *nl* with an accuracy of at least 5 *nl* .

2. The operating principle and structure of the MHD micropump

2.1 An operating principle of MHD micropump

A typical MHD (magnetohydrodynamic) micropump has been reported in which the conducting fluid contains ions in the microchannel of the MHD micropump subjected to the Lorentz force induced in the direction perpendicular to both magnetic and electric fields. The Lorentz force is the pumping source for electrically conducting liquid with conductivity. To give a more detailed explanation, Fig. 1(a) shows the basic principle of the MHD micropump. In a hexahedral microchannel with transverse current density (J_z) and perpendicular to transverse magnetic flux density(B_y), the Lorentz forces(F_x) can be written as follows.

$$\vec{F}_x = \vec{J}_z \times \vec{B}_y$$

The schematic of a simple MHD micropump is shown in Fig. 1(b). Lorentz force is induced in the direction perpendicular to both magnetic flux density and current density vector and thus, the working fluid in the microchannel flows into +x-direction by the resulting Lorentz force. One thing to note is that the working fluid used in the MHD micropump is limited to electrically conducting liquid with conductivity of the order of 1 S/m or higher, such as NaCl. In view of the operating principle, the MHD micropumps have several advantages of continuous flow forces and bi-directional pumping capability over other non-mechanical micropumps. In addition, depending on the design of the MHD micropump, it allows for multiple and independently controlled pumps to be integrated on a single silicon chip for producing complex microfluidic systems.

Fig. 2 is the recently studied schematic diagram of the MHD micropump fabricated by POSTECH (Pohang University of Science and Technology)[7]. To allow a certain level of currents to working fluid in a microchannel, the MHD micropump must have electrodes on the upside and the bottom surfaces of the microchannel. When depositing electrodes on those surfaces, one structural importance is that the oxide layer (SiO_2) must be between (+) electrode and (–) electrode so that the current can flow through only the conducting fluid. Si wafer itself is electrical conductivity, which brings about discharge in the absence of an oxide layer between two electrodes when voltage is applied. The oxide layer (SiO_2) is the widely used

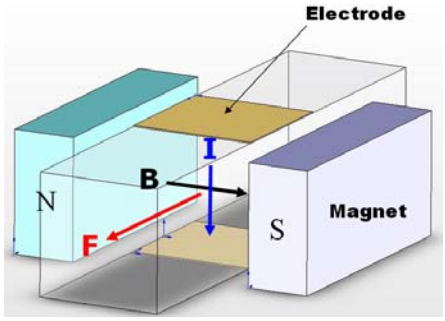

(a) 3-dimensional diagram

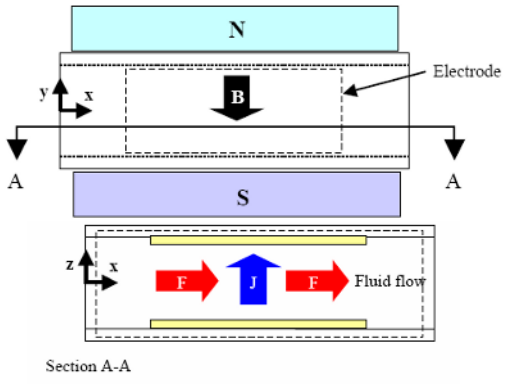

(b) 2-dimensional diagram

Fig. 1. Schematic of the actuation principle of the MHD micropump in which driving force is Lorentz force.

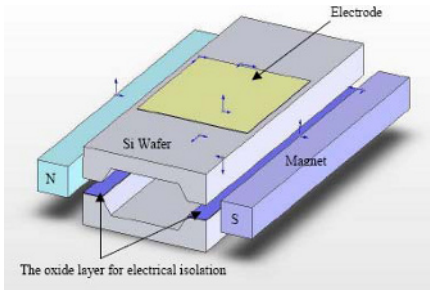

Fig. 2. Schematic of the MHD micropump presented by POSTECH[7].

substance for electrical isolation layers. To apply magnetic fields from the outside, a permanent magnet with a certain level of magnetic flux density is on both sides of the MHD micropump device.

2.2 The structure of the MHD micropump with side-walled electrodes

The MHD micropump with side-walled electrodes

proposed from this paper is illustrated in Fig. 3, which is composed of the microchannel, side-wall electrodes and the permanent magnet. The microchannel is formed through the wet etching process on silicon wafer. Side-wall electrodes are deposited by thermal oxidation. To maintain the electrical isolation on both electrodes and facilitate the proper flow of working fluid, a thickness of approximately 0.5 ㎛ of oxide layer was formed within the microchannel. As a result, the microchannel was fabricated 30mm in length, 100 ㎛ in depth and 100 ㎛ in width. The dimension of the whole MHD micropump device is 40mm × 25mm × 1mm. The permanent magnet has diameter of 15mm and heights of 10mm and 5mm, respectively. An acryl-made frame fixes both the MHD micropump device and permanent magnet 5mm away from each other. The MHD micropump with side-walled electrodes, apart from other conventional MHD micropumps, has metal electrodes deposited on side-walls of microchannel running working fluid, which makes the fabrication process simple. As the permanent magnet is placed on the bottom of the MHD micropump device to induce external magnetic field, it is easy to miniaturize the size of the completed micropump.

3. The fabrication process of the MHD micropump

The MHD micropump consists of the anisotropic bulk-etched microchannel, the side-walled electrodes, and the single permanent magnet (Nd-Fe-B). The micro-channel of the MHD micropump has width of 1 mm, depth of 0.1mm, and length of 30mm. The cross-section of the microchannel has the shape of a trapezoid by anisotropic etching. A thin oxide layer is then formed for electrical isolation. Metal electrodes (5000 Å Al) are deposited on to the side-walls of the channel by using thermal evaporation and shadow mask patterning. The fabricated silicon wafer is then anodically bonded with Pyrex glass. Before the bonding process, four holes for fluidic input, output and electrical contact were drilled through the EDM (electro discharge machining) process. Fig. 4 shows the fabrication process.

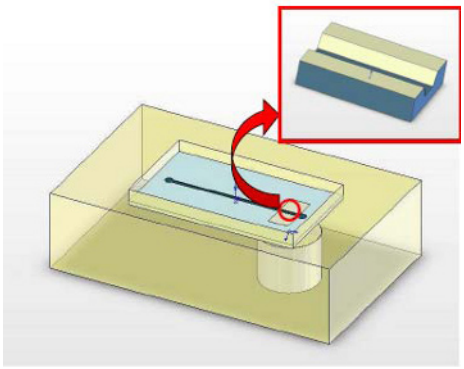

Fig. 3. The MHD micropump with the side walled electrodes.

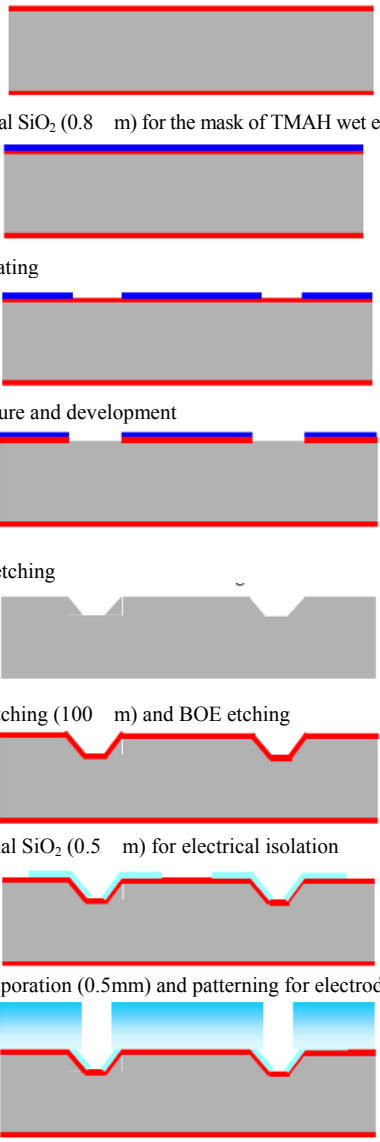

Fig. 4. The fabrication process flow for the proposed MHD micropump.

It is a relatively simple process with a photomask. It started with double polished 525-㎛-thick p-type (100) 4-inch Si wafers. Initial 0.8-㎛-thick thermal SiO2 was grown as etching mask at 1100°C in wet atmosphere for 100 min. After the photolithography process, the 100um depth microchannel was defined by wet etching in 25 wt.% tetramethylammonium hydroxide (TMAH) at 78°C for 200min (etch rate : 0.5 ㎛/min). Remaining oxides were then removed and an oxide layer of 0.5 ㎛ thickness through a thermal evaporation was grown for electrical isolation at 1100°C in wet atmosphere for 60min. Al electrodes are then deposited on to the side walls of the microchannel by thermal evaporation. To pattern Al electrodes, a shadow mask was used. Inlet, outlet and electric wire holes were fabricated on Pyrex glass through EDM (electro discharge machining). The silicon wafer was then exposed to the anodic bonding process with Pyrex glass. After the completion of the anodic bonding process, the MHD micropump device was completed through a dicing saw process. Fig. 5 shows a photograph of a practically fabricated MHD micropump.

Table 1 gives the list for the dimensions and hydraulic diameter of the microchannel within the fabricated structure.

4. The simulation of fully developed laminar flow for the MHD micropump

4.1 Fundamental analysis

4.1.1 Electromagnetic theory

In the MHD micropump, the pumping forces originate from the electromagnetic Lorentz force induced by the applied electric currents. The basic principle is to apply the electric current across the channel filled with electrically conducting liquid and a DC magnetic field orthogonal to the currents via permanent magnet. The governing equations of the Lorentz force are derived with the assumption that steady-state fields with constant magnetic and electric properties are on the working fluid. Hence, the Lorentz force($\vec{F}$) can be written as follows.

$$\vec{F} = \vec{J} \times \vec{B} \tag{1}$$

where $\vec{B}$ is magnetic flux density vector, $\vec{J}$ being current density vector, and $\vec{J}$ is derived based upon the Ohm's Law below.

$$\vec{J} = \sigma(\vec{E} + \vec{V} \times \vec{B}) \tag{2}$$

where $\vec{E}$ represents the electric field intensity vector, σ being electrical conductivity of the conducting liquid, and V being flow velocity vector.

Table 1. The dimensions of the microchannel in the micropump.

Width(㎛)	Depth(㎛)	D_h(㎛)
1000	100	181

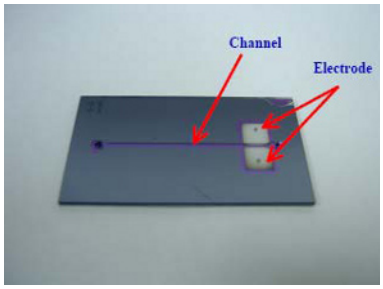

Fig. 5. Photograph of the fabricated MHD micropump.

4.1.2 Fluid dynamics theory

According to the study published on the microchannel flows[10], the experimental results have indicated that the flow rates were approximately the same as the predictions given by the Poiseuille flow conditions on micro-tubes with relatively large diameters(>100 ㎛). However, as the Reynolds number increased, a significant pressure gradient increase was observed while the conventional laminar theory would predict less increase. The rationale is that the increase in pressure gradient may be due to either an early transition from laminar flow to turbulent flow or the surface roughness of the micro-tubes being significant. In conclusion, the conventional laminar theory is still applicable for the microchannel flow in relatively large channels; but the deviations increase along with the reduction of the channel size. Since the Reynolds number in the microchannel is assumed to be small, the flow field in the MHD micropump is treated as steady state, incompressible, and fully developed laminar flow condition. And the y and z axis of the flow velocity are also assumed to be zero. Based upon the above assumption, the axial flow velocity (u) is invariant along the x direction such that u = u(y, z) and v = w = 0. On the other hand, the effect of surface tension is neglected since the microchannel is assumed to be filled with fluids. For the

simplified flow field, the governing equations can be written as follows:

Continuity equation

$$\frac{\partial u}{\partial x} = 0 \tag{3}$$

Momentum equations

$$-\frac{\partial p}{\partial x} + \mu\left(\frac{\partial^2 u}{\partial y^2} + \frac{\partial^2 u}{\partial z^2}\right) = 0$$

$$-\frac{\partial p}{\partial y} = -\frac{\partial p}{\partial z} = 0 \tag{4}$$

Where μ . is the dynamic viscosity of the fluid.

In the microchannel, under electromagnetic interactions, the Lorentz forces acting on the fluid particles are considered as hydrostatic pressure head uniformly distributed over the entire channel region; hence, it is expressed as follows:

$$\frac{\Delta p}{L} = -\frac{\partial p}{\partial x} \tag{5}$$

where Δp is the pressure head along the channel with length L given by the cross products of the current density vector and magnetic field density vector. That is

$$\Delta p = \left(\vec{J} \times \vec{B}\right) L_p \tag{6}$$

where L_p is the length of electrode. From Eqs. (2), (5) and (6), the pressure gradient generated by the applied DC electric and magnetic fields in the flow channel can be obtained. After the pressure gradient is substituted into Eq. (4), the momentum equation is rewritten as Eq. (7).

$$\left(\frac{\sigma B E L_p}{\mu L} - \frac{\sigma B^2 L_p}{\mu L} u\right) + \frac{\partial^2 u}{\partial y^2} + \frac{\partial^2 u}{\partial z^2} = 0 \tag{7}$$

Hence, the volumetric flow rate (Q) based upon the integral of cross sectional microchannel area is then given by Eq. (8).

$$Q = \iint u(y,z)\,dydz \tag{8}$$

Finally, the numerical central difference scheme based upon the finite difference method is employed for solving the velocity profile across the channel. Parameters for the applied magnetic fields and electric currents with specific channel depths and widths have been adjusted for the assessments of the performance of the micropump.

4.2 Results from the simulation with finite difference method

The electrically conducting fluid, PBS solution, is employed as the working medium for numerically simulating the DC MHD micropump. The pertinent material properties of PBS solution are summarized in Table 2. In addition, the geometric dimensions and applied fields needed for the numerical simulations are listed in Table 3.

Table 2. The material properties for PBS solution.

	Density, $\rho\ (kg/m^3)$	Conductivity, $\sigma\ (S/m)$	Viscosity, $\mu\ (Pa\ s)$	Relative permeability	Relative permittivity
PBS solution	1000	1.5	6×10^{-4}	1	72

Table 3. Parameters for numerical simulation.

Parameter	Value
Channel depth(㎜)	0.1
Channel width (㎜)	1
Channel length (㎜)	30
Electrode length, L_p (㎜)	5, 7.5, 10
Magnetic flux density, B (Gauss)	4900, 3300
Input current, I (㎃)	0 ~ 10

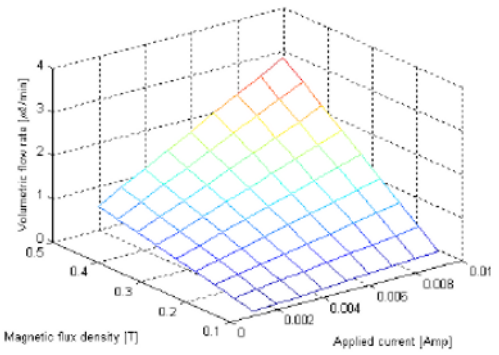

Fig. 6. Simulation results for the flow rates of PBS solution as a function of current and magnetic fulux density.

Fig. 6 shows the simulated results for the variations of volumetric flow rates of MHD micropump with 10000 ㎛ length of electrode under various operation currents and magnetic flux densities.

The numerical analysis based upon the finite difference method has been implemented through MATLAB. The flow rate is 3.22 ㎕/min when the magnetic flux density is 0.49T (4900 Gauss) with the applied current of 0.9mA. The flow rate can be increased to improve the performance of the MHD micropump if the magnitude of the magnetic field or the applied current is increased. It is noted from Fig. 6 that the flow rate of PBS solution increases linearly with the magnitude of the applied current and the magnetic flux density. Fig. 7 depicts that the volumetric flow rate typically increases with the applied current and magnetic flux density.

The calculated results published by other researchers using Poiseuille's Law[11, 12] are also illustrated in the figures and compared with the numerically analyzed results implemented through MATLAB based upon the FDM (finite difference method). The reason that there are discrepancies between them is because the Poiseuille law neglects the frictional effects on both sidewalls and one-dimensional laminar flow model simplified by the Poiseuille law would be rough.

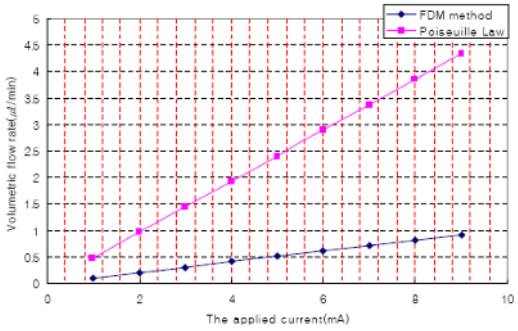

(a) The flow rates with applied currents

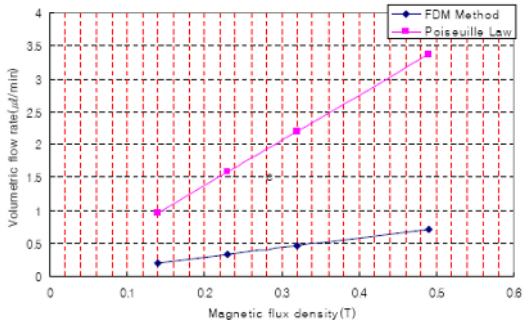

(b) The flow rates with magnetic flux densities

Fig. 7. Comparison of the simulated flow rates and the results calculated by the Poiseuille law.

4.3 Results from the simulation using commercial code CFD-ACE

The 2-D microchannel structure was modeled as shown in Fig. 8 to primarily consider the dimensions of the MHD micropump.

Initial temperature was 300K in the microchannel, wall, and working fluid and the reference pressure was set as 100000N/㎡. To specify the volume condition properties of working fluid, Table 2 was provided as reference. The electrical conductivity would be the most important data since the working fluid is electrolytic. To analyze the effect of magnetic field, other variables (pressure, the applied current between electrodes, the characteristics of working fluid- density, viscosity, relative permittivity, relative permeability, electrical conductivity) remained constant. Fig. 9 shows the flow velocity profile in the microchannel with 5000 ㎛ length of electrode under 4900G and 3300G of magnetic flux density when the applied current was fixed at 0.4mA.

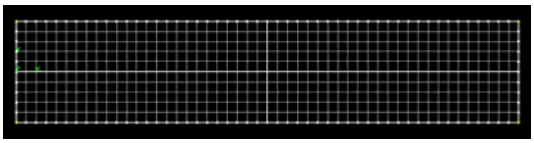

Fig. 8. Modeling geometry for the MHD pump.

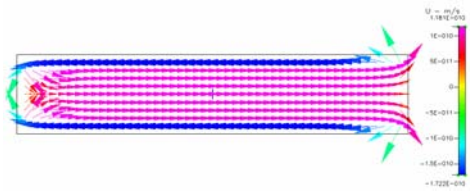

(a) 4900 G of magnetic flux density

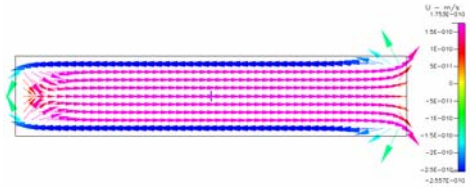

(b) 3300 G of magnetic flux density

Fig. 9. Flow velocity profile with 0.4mA of the applied current.

The maximum flow velocity at 4900G of magnetic flux density was higher than that at 3300G. The simulation results show that the volumetric flow rate is proportional to the magnetic flux density. To analyze the effect of electric field, other variables (pressure, magnetic flux density, the properties of working fluid- density, viscosity, relative permittivity, relative permeability, electrical conductivity) were uniformly fixed.

5. Performance of the MHD micropump

The performance of the MHD micropump can be determined through the magnitude of the electric and magnetic fields. As Lorentz force, which induces forces to working fluid, is expressed by the cross-product of the electric current and the magnetic flux density, better efficiency can be achieved by inducing the higher electric and magnetic fields. In order to find the performance of MHD micropump, an experiment for measuring the flow rate with the variation of the electric and magnetic fields was performed.

5.1 Measurement set-up2.2 reference

Fig. 10(a) shows the test set-up for measuring flow rates as the applied current changes. A plate made of acryl was used for maintaining 5mm distance between the MHD micropump device and the permanent magnet. A capillary tube was fixed to the supporter out of acryl. Hi-scope (KH-220, HiRox) was used to observe and record the process. The flow rate was calculated from the moving distance of the working fluid with time. A Hi-scope was positioned above the capillary tube located in the outlet. The Hi-scope has a CCD camera, which is connected to a computer with video capture software. As the working fluid for the actual experiment was applied to the analysis of protein, PBS buffer solution was used as medium for the fixation of protein. Fig. 10(b) shows the photograph of the measurement set-up in the real experiment. Steady state currents were measured according to the applied voltage from the side-wall electrodes under the condition that the microchannel is filled with working fluid. In the EHD micropump, the IV curve has a high nonlinearity, when high DC voltage currents is applied to working fluids[1]. However, the IV curve shows linearity in the MHD micropump because it is operated with a relatively lower voltage compared to EHD micropump.

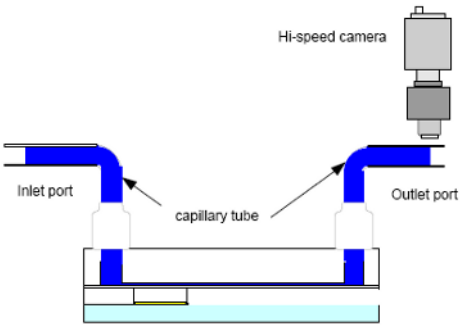

(a) Schematic diagram

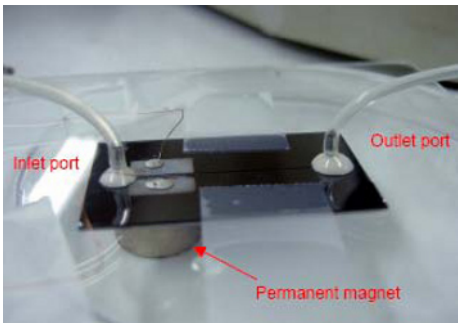

(b) Photograph of the setup

Fig. 10. The experimental setup for measuring flow rates.

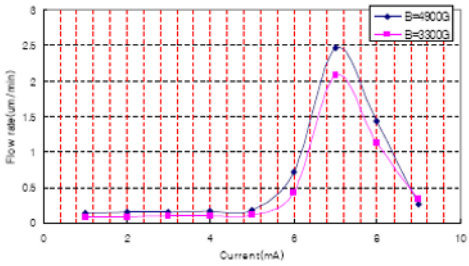

Fig. 11. The volumetric flow rate due to applied current.

5.2 Results of the volumetric flow rate from experiment

To actually apply to microfluidic system, one conducting liquid, namely, PBS buffer solution was employed as the working fluid. PBS buffer solution is composed of Sodium Phosphate (0.01M), NaCl (0.138M), and KCl (0.0027M). For the measurement of the flow rate as shown in Fig. 10, the voltages were applied to the working fluid. It has the same height in both the tubes of input and output during the experiments in order to get the effect of only the Lorentz force. Fig. 11 indicates the volumetric flow rate when a current from 1 to 9 mA is applied.

At B = 4900 G and B = 3300 G, the flow rate was measured as currents gradually went up with 1mA interval. The curve can be divided into three different regions: the linear low-field region (α. zone), the steeply increasing region (β. zone), and the steeply decreasing region (γ. zone). The linear low-field region (α. zone) is stable. Bubbles are hardly generated in the microchannel of the MHD micropump. The working fluid in stable state becomes the continuous flow by the Lorentz force caused from the magnetic and electric fields.

In the steeply increasing region (β. zone), the bubbles are generated in the conducting liquid over a current of 5mA. They are generated more frequently and become larger as the current increases. The measured flow rate is also higher than the theoretical one because of the bubble generation. The bubble is created by electrolysis caused by the interaction between Al electrodes and PBS solution. Bubble gas generated by electrolysis is presumed to be O_2 from a substance constituting PBS solution. Fig. 12 shows the bubble generation in the microchannel. Fig. 12(a) is the microscope-captured image of α. zone in the continuous flow, before bubble generating. Fig. 12(b) shows the bubble generating state with an applied current of more than 6mA in the β. zone where bubbles are generated.

After passing the maximum flow rate point by bubble generation, a steeply decreasing region (γ. zone) of the flow rate is observed, which is caused by the electrode degradation (or corrosion) due to electro-chemical reaction. Fig. 13 shows the moving distance of working fluid per unit time in each flow region (α, β, γ. zone), in which $\Delta l_2 > \Delta l_3 > \Delta l_1$ as expected in Fig. 11. For the application of microfluidic system, the bubble generating band, i.e., unstable regions (β. zone and γ. zone), should be avoided.

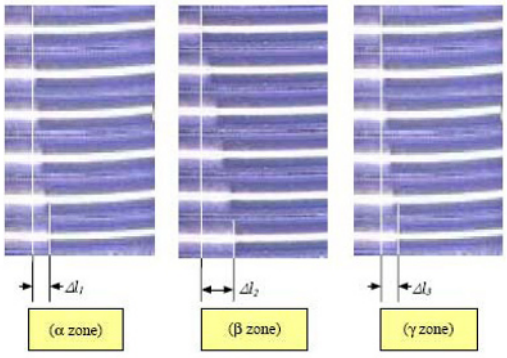

Fig. 12. The captured images of the PBS solution flow in the capillary tube.

5.3 Discussions for the experimental verification

The Poiseuille flow theory model neglects the frictional effects in both sidewalls and the effect of electric field based on the length of electrode because of the one-dimension analysis. On the contrary, the numerical simulations conducted by the FDM (finite difference method) and CFD-ACE software show that the channel dimensions and the induced Lorentz force have significant influences on the flow velocity profile because of the two-dimensional laminar flow model. Fig. 14 shows the comparisons of the results among the experiment, the numerical simulation, and the calculation by the Poiseuille Law.

The numerical results with FDM are in better agreement with the experimental results as compared to the calculation results by the Poiseuille Law. In conclusion, the Poiseuille law, based upon one-dimensional fully developed laminar flow, cannot take account of the frictional effects of the channel side walls and the direct substitution of the Lorentz

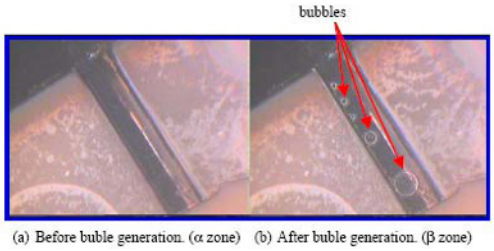

Fig. 13. Photograph of the microchannel in the micropump before and after bubble generation.

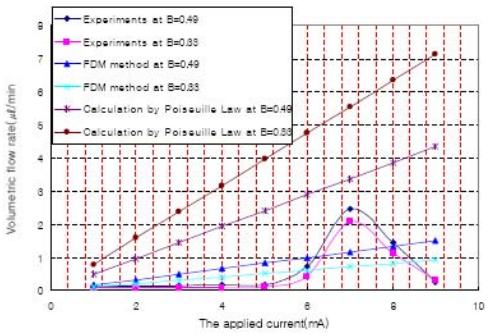

Fig. 14. Comparison of the experimental results, the numerically analyzed results (FDM method) and the calculation results by Poiseuille law.

force into the analytic solutions of the momentum equations would result in the deviations between numerical and experimental results because the effects of induced current generated from the fluid passing through magnetic field and the induced reverse Lorentz force are not accounted for in the formulation. In addition, the reduced volume by the bubble generation in the microchannel causes higher flow rates than numerical values.

6. Conclusions

The MHD micropump with side-walled electrodes has been fabricated. A numerical simulation for modeling the MHD micropump based on fully developed two-dimensional laminar channel flow was used to predict the operating characteristics. In order to consider the induced Lorentz force generated in the conducting liquid under the applied electric and magnetic fields, the formulations of the Lorentz force were substituted into the source terms of the momentum equations instead of the analytic solutions. The simulated volumetric flow rates, solved by means of a finite difference method, were compared with the experimental results. In the actual performance experiment of the MHD micropump, the reduced volume by the bubble generation in the microchannel caused the higher flow rates than numerical values. The maximum flow rate of the MHD micropump shows 0.3 ㎛/min to the low current region(<5mA) in stable region. In the numerical simulation, the characteristics of the flow rate were analyzed. To get the effect of the maximum flow rates by the magnetic flux intensity, a permanent magnet with 4900G of magnetic flux density must be closer to the MHD micropump device to get up to 4900G. The effect of electric field on flow rates has been studied. The flow rate is slowly increased in the low current area. It is suddenly increased by the bubble generation in the high current region. After the increase of the flow rate, a region, in which it suddenly goes down, can be observed. It could be explained by the corrosion of Al electrode which later breaks down the performance of the MHD micropump. To yield a better effect of the flow rate by electric field, bubble generation needs to be reduced In order to get rid of the generation of the bubble gas due to electrolysis of PBS solution with Al electrodes, Au electrode should be used. In addition, instead of using DC current and DC magnetic field (permanent magnet), an AC current of sufficiently high frequency and AC magnetic field from an electromagnet can be utilized. After all, the MHD micropump has many advantages over other types of micropumps, such as bi-directional pumping ability, simple fabrication, and the ability to handle the protein-fixing medium conducting liquid. Therefore, the suggested micropump could be used for μ-TAS (micro total analysis system) or drug delivery systems for the analysis of protein.

Acknowledgment

This study was supported by the Korea Research Foundation Grant (KRF-2005-005-D00003).

References

[1] M. Richter, J. Kruckow, J. Weidhaas, M. Wackerle, A. Drost, U. Schaber, M. Schwan and K. Kühl, *Batch fabrication of silicon micropumps*, in Proceedings of the Transducers '01/Eurosensors XV, Munich, Germany (2001) 936-939.

[2] S. F. Bart, M. Mehregany, L. S. Tavrow and J. H. Lang, *Microfabricated electrohydrodynamic pumps*, Transducers '89, Book of Abstracts, Montreux, Switzerland (1989) 113.

[3] A. Richter, H. Sandmaier, *An electrohydrodynamic micropump*, in Proceedings of the MEMS '90, Napa Valley, USA (1990) 99-104.

[4] A. Richter, A. Plettner, K. A. Hoffmann, H. Sandmaier, *Electrohydrodynamic pumping and flow measurement*, in Proceedings of the MEMS '91, Nara Japan 30 (1991) 271-276.

[5] R. M. Moroney, R. M. White and R. T. Howe, *Ultrasonically induced microtransport*, in Proceedings of the MEMS '91, Nara, Japan, 30 (1991) 277-282.

[6] J. C. Rife, M. I. Bell, J. S. Horwitz, M. N. Kabler, R. C. Y. Auyeung and W. J. Kim, *Miniature valveless ultrasonic pumps and mixers*, Sensors Actuators 86 (2000) 135-140.

[7] J. Jang and S. S. Lee, *Theoretical and experimental study of MHD(magnetohydrodynamic) micropump*, Sensors Actuators 80 (2000) 84-89.

[8] S. Böhm, *The comprehensive integration of microdialysis membranes and silicon censors*, Ph.D. Thesis, University of Twente, The Netherlands (2000).

[9] G. J. Kellogg, T. E. Arnold, B. L. Carvalho, D. C. Duffy and N. F. Sheppard Jr., in A van den Berg, et al. (Eds.), *Micro Total Analysis Systems 2000*,

Kluwer Academic Publishers, Dordrecht (2000) 239-242.
[10] Pfahler, J., Harley, J., Bau, H. H., Zemel, J., *Liquid and gas transport in small channels*. ASME DSC, 19 (1990) 149-157.
[11] Leonardo Di G. Sigalotti, Jaime Klapp, Eloy Sira, Yasmin Meleán, Anwar Hasmy, *SPH simulations of time-dependent Poiseuille flow at low Reynolds numbers*, Journal of Computational Physics, 191 (2) (2003) 622-638.
[12] P. Filip and J. David, *Axial Couette–Poiseuille flow of power-law viscoplastic fluids in concentric annuli*, Journal of Petroleum Science and Engineering, 40 (3-4) (2003) 111-119.

Bumkyoo Choi received a B.S. degree in mechanical engineering, M.S. in mechanical design engineering from Seoul National University, Seoul, Korea in 1981 and 1983 respectively, and PhD in engineering mechanics from the University of Wisconsin, Madison in 1992. From 1992 to 1994, he was a technical staff member of CXrL (Center of X-ray Lithography) in the University of Wisconsin where he developed a computer code for thermal modeling of X-ray mask membrane during synchrotron radiation. He is currently a professor in the Dept. of Mechanical Engineering of Sogang Univ., Seoul, Korea. His research interest includes microelectromechanical system (MEMS), micromatching and microfabrication technologies, and modeling issues.

Sangsoo Lim received a B.S. degree in mechanical engineering from Sogang University, Seoul ,Korea in 2005. He currently works at Hyundai Motors.